

Electronic spectroscopy of the $\tilde{A}^1A'' \leftrightarrow \tilde{X}^1A'$ system of CDCl

Chong Tao, Calvin Mukarakate, Scott A. Reid *

Department of Chemistry, Marquette University, Milwaukee, WI 53201-1881, USA

Received 8 November 2006; in revised form 30 November 2006

Available online 13 December 2006

Abstract

We report fluorescence excitation and single vibronic level emission spectra of the $\tilde{A}^1A'' \leftrightarrow \tilde{X}^1A'$ system of CDCl in the 500–740 nm region, measured under jet-cooled conditions using a pulsed discharge source. A total of 29 cold bands involving the pure bending levels 2_0^n ($n = 2-11$), C–D stretching fundamental (1_0^1), and combination bands $2_0^2 3_0^1$ ($n = 2-10$), $2_0^2 3_0^2$ ($n = 9$), $1_0^1 2_0^n$ ($n = 2-8$), and $1_0^1 2_0^2 3_0^1$ ($n = 7$) were observed; most of these are reported here for the first time. Rotational analysis typically yielded band origins and rotational constants for both isotopomers (CD^{35}Cl , CD^{37}Cl). The derived \tilde{A}^1A'' vibrational intervals are combined with previous studies at lower energy to determine excited state barriers to linearity for the 2^n , $2^n 3^1$, and $1^1 2^n$ progressions. The \tilde{A}^1A'' state C–D stretching frequency (2229.6 cm^{-1}) is determined here for the first time, in excellent agreement with *ab initio* theory. Following our observation of new bands in this system, we obtained single vibronic level (SVL) emission spectra which probe the vibrational structure of the \tilde{X}^1A' state up to $\sim 8000 \text{ cm}^{-1}$ above the vibrationless level. The total number of \tilde{X}^1A' and \tilde{a}^3A'' levels observed is more than twice that previously reported, and a complete set of Dunham parameters was determined for the \tilde{X}^1A' state of CD^{35}Cl and CD^{37}Cl . Comparisons with previous experimental and recent high level *ab initio* studies are reported. Our results shed new light on the vibrational structure of the \tilde{X}^1A' , \tilde{A}^1A'' , and \tilde{a}^3A'' states of CDCl, and, more generally, spin–orbit coupling in the monohalocarbenes.

© 2007 Elsevier Inc. All rights reserved.

1. Introduction

Carbenes are important intermediates in various chemical processes including organic chemistry, combustion and atmospheric chemistry [1–6]. The divalent carbon gives rise to energetically similar singlet and triplet states, with very different reactivities. Therefore, understanding carbene chemistry requires knowledge of the singlet–triplet gap, ΔE_{ST} . Recently, much progress has been made in our understanding of the electronic structure and spectroscopy of simple carbenes such as CH_2 and the monohalocarbenes CHX ($\text{X} = \text{F}, \text{Cl}, \text{Br}, \text{I}$); see Refs. [7,8] for a detailed list of references. For the monohalocarbenes, the two low lying singlet states (\tilde{A}^1A'' , \tilde{X}^1A') correlate with a $^1\Delta$ state in the linear configuration, forming a Renner–Teller (RT) pair, and the spectra are thus complicated by RT and spin–orbit

interactions involving the lowest three potential energy surfaces.

Building upon the seminal work of Merer and Travis in the 1960's [9,10], and later work from the groups of Hirota [11–18], Sears [19–33], Kable [34–36], and Chang [37–43], our group has recently undertaken a systematic study of the monohalocarbenes CHF, CHCl, CHBr and their deuterated isotopomers, using a variety of methods including fluorescence excitation spectroscopy, lifetime measurements, polarization and Zeeman quantum beat spectroscopy, and single vibronic level emission spectroscopy [8,44–54]. Most recently, we reported comprehensive surveys of the $\tilde{A}^1A'' \leftrightarrow \tilde{X}^1A'$ system of CHBr, CDBr, and CHCl using fluorescence excitation and single vibronic level (SVL) emission spectroscopy [8,53,54]. In each case we recorded and analyzed many new cold bands, and reported the first measurement of the \tilde{A}^1A'' state C–H stretching frequencies following the observation of bands in the progressions $1_0^1 2_0^n$ and $1_0^1 2_0^2 3_0^m$ [36,46,52]. Exploiting these as pump transitions in SVL emission spectroscopy,

* Corresponding author. Fax: +1 414 288 766.

E-mail address: scott.reid@mu.edu (S.A. Reid).

we examined the vibrational level structure up to $\sim 9000\text{ cm}^{-1}$ above the vibronic origin of \tilde{X}^1A' , reporting many previously unobserved levels in both the \tilde{X}^1A' and \tilde{a}^3A'' states and probing spin–orbit mixing in these systems in new detail. For CHCl, we obtained SVL emission spectra from excited state levels with $K'_a = 1$ and determined the effective rotational constant $(A - B) = 26(2)\text{ cm}^{-1}$ of the triplet origin [53], in excellent agreement with *ab initio* theory.

In this paper, we extend our studies to CDCl. Experimental studies of the spectroscopy of CDCl began with the work of Merer and Travis [9], who reported absorption spectra of the $\tilde{A}^1A'' \leftarrow \tilde{X}^1A'$ system which showed a long progression in the bending mode. Interestingly, combination bands involving the C–Cl stretch, which had been observed for CHCl, were not observed for CDCl. Later, Sears and co-workers examined the 2_0^1 band under high resolution, determining precise rotational constants for the upper and lower states [28]. Chang and co-workers reported emission spectra of CHCl and CDCl which probed the vibrational structure of the \tilde{X}^1A' state and spin–orbit mixing with \tilde{a}^3A'' [37,40,42].

Here, we report new LIF spectra of jet-cooled CDCl in the 500–740 nm region. Our measurements yielded rotationally resolved spectra for 29 cold bands, most of which are observed here for the first time. We were typically able to analyze bands for both (^{35}Cl , ^{37}Cl) isotopomers, and report on the vibrational state dependence of the isotope shift in the excited state. We also report the first observation of bands containing C–D stretching excitation, from which the \tilde{A} state C–D stretching frequency was determined, in excellent agreement with recent *ab initio* calculations [31]. Following our observation of new bands in this system, we obtained a series of single vibronic level (SVL) emission spectra which probe the vibrational structure of the \tilde{X}^1A' and \tilde{a}^3A'' states up to $\sim 8000\text{ cm}^{-1}$ above the vibrationless level of the \tilde{X}^1A' state. As in our previous study of CHCl [53], we observe many previously unassigned levels in both the \tilde{X}^1A' and \tilde{a}^3A'' manifolds. A detailed comparison of vibrational term energies for both states is made with the predictions of two recent *ab initio* studies [31,55], and a Dunham expansion fit to the observed term energies was used to determine a complete set of \tilde{X}^1A' state vibrational parameters for both isotopomers.

1.1. Experimental section

The apparatus, pulsed discharge nozzle, and data acquisition procedures are identical to those used in previous studies of CHF, CDF, CHBr, CDBr, and CHCl [8,44–54], and, therefore, only the important differences will be highlighted. The carbene CDCl was produced using a pulsed electrical discharge through a ~ 1 –2% mixture of CD_2Cl_2 (Cambridge Isotope Labs, 99.9 atom % of D) seeded in high purity He. The precursor was kept in a temperature controlled stainless steel bubbler, through which pure He gas was passed at a pressure of 2–4 bar.

In analyzing the fluorescence excitation spectra, transition frequencies were fit to a standard asymmetric top Hamiltonian using a least squares routine in the AsyrotWin program package of Judge and Clouthier [56], incorporating the ground state rotational constants determined in the high resolution study of Lin et al. [28]. The transition frequencies were calibrated to vacuum wavenumbers based on optogalvanic lines recorded using a Fe:Ne hollow cathode lamp.

2. Results and discussion

2.1. Fluorescence excitation spectra

The $\tilde{A}^1A'' \leftrightarrow \tilde{X}^1A'$ spectra of CDCl are qualitatively similar to CHCl, with one important difference. In CHCl, combination bands involving the CH stretch and CCl stretch were only observed in excitation at higher energy [9,42,45,53], however, in CDCl we observe more extensive activity in the $2_0^n 3_0^1$ and $1_0^1 2_0^n$ progressions. We thus obtained and rotationally analyzed fluorescence excitation spectra of 29 cold bands involving the pure bending levels 2_0^n with $n = 2$ –11, C–D stretching fundamental (1_0^1), and combination bands $2_0^n 3_0^1$ ($n = 2$ –10), $2_0^n 3_0^2$ ($n = 9$), $1_0^1 2_0^n$ ($n = 2$ –8), and $1_0^1 2_0^n 3_0^1$ ($n = 7$) in the $\tilde{A}^1A'' \leftarrow \tilde{X}^1A'$ system; Fig. 1 presents a survey scan of this system. The fitted parameters are listed in Table 1, which also includes the CD^{35}Cl term

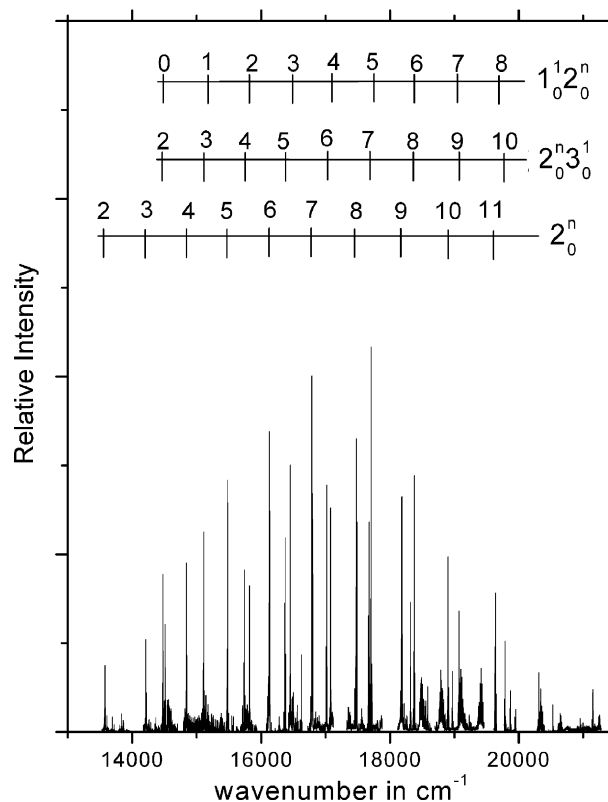


Fig. 1. Survey fluorescence excitation spectrum of the $\tilde{A}^1A'' \leftarrow \tilde{X}^1A'$ system of CDCl. Assignments are noted for the major progressions. The relative intensities are un-normalized between spectra or to laser power, and thus must be considered approximate.

Table 1
Fit parameters (in cm^{-1}) for the CDCl ($\tilde{A}'A'' \leftarrow \tilde{X}'A'$) bands measured in this work

Band	Isotope	T (exp.) ^a	T (calc.) ^b	$(B' + C')/2$	N^c	σ^d
2_0^2	^{37}Cl	13576.87(2)	13571.2	—	12	0.02
	^{35}Cl	13578.38(4)		0.5344(7)		
2_0^3	^{37}Cl	14213.22(24)	14205.3	0.5233(42)	6	0.07
	^{35}Cl	14214.46(16)		0.5441(44)		
$2_0^2 3_0^1$	^{37}Cl	14470.10(12)	14530.7	0.5231(19)	7	0.05
	^{35}Cl	14478.18(6)		0.5294(14)		
1_0^1	^{37}Cl	14510.98(20)	14503.8	—	14	0.08
	^{35}Cl	14511.99(14)		0.5411(49)		
2_0^4	^{37}Cl	14843.09(20)	14837.0	—	12	0.04
	^{35}Cl	14845.44(6)		0.5379(17)		
$2_0^3 3_0^1$	^{37}Cl	15103.80(10)	15166.0	0.5198(33)	7	0.03
	^{35}Cl	15112.17(7)		0.5318(21)		
2_0^5	^{37}Cl	15476.60(20)	—	—	18	0.04
	^{35}Cl	15479.65(5)		0.5362(5)		
$2_0^4 3_0^1$	^{37}Cl	15733.57(10)	—	0.5218(22)	10	0.06
	^{35}Cl	15742.28(11)		0.5365(20)		
$1_0^1 2_0^2$	^{37}Cl	15820.37(7)	—	0.5308(24)	4	0.02
	^{35}Cl	15822.14(4)		0.5319(4)		
2_0^6	^{37}Cl	16123.49(20)	—	—	14	0.04
	^{35}Cl	16126.87(6)		0.5361(9)		
$2_0^5 3_0^1$	^{37}Cl	16366.97(7)	—	0.5237(13)	11	0.04
	^{35}Cl	16376.18(9)		0.5327(32)		
$1_0^1 2_0^3$	^{37}Cl	16452.70(20)	—	—	16	0.04
	^{35}Cl	16454.92(6)		0.5324(15)		
2_0^7	^{37}Cl	16788.39(20)	—	—	25	0.05
	^{35}Cl	16792.80(4)		0.5376(4)		
$2_0^6 3_0^1$	^{37}Cl	17011.46(19)	—	0.5248(30)	6	0.09
	^{35}Cl	17020.90(7)		0.5320(10)		
$1_0^1 2_0^4$	^{37}Cl	17077.65(20)	—	—	14	0.04
	^{35}Cl	17080.72(6)		0.5330(17)		
2_0^8	^{37}Cl	17474.46(2)	—	0.5305(5)	6	0.01
	^{35}Cl	17479.33(3)		0.5388(6)		
$2_0^7 3_0^1$	^{37}Cl	17669.32(3)	—	0.5252(5)	14	0.03
	^{35}Cl	17677.43(2)		0.5330(3)		
$1_0^1 2_0^5$	^{37}Cl	17707.01(7)	—	0.5252(17)	10	0.03
	^{35}Cl	17712.05(8)		0.5295(11)		
2_0^9	^{37}Cl	18178.22(20)	—	—	15	0.07
	^{35}Cl	18183.93(9)		0.5435(22)		
$1_0^1 2_0^6$	^{37}Cl	18319.46(3)	—	0.5273(6)	13	0.02
	^{35}Cl	18323.87(3)		0.5349(4)		
$2_0^8 3_0^1$	^{37}Cl	18367.47(3)	—	0.5262(9)	12	0.02
	^{35}Cl	18377.49(3)		0.5346(1)		
2_0^{10}	^{37}Cl	18897.90(8)	—	0.5352(23)	12	0.05
	^{35}Cl	18904.89(2)		0.5408(4)		
$1_0^1 2_0^7$	^{37}Cl	18967.26(3)	—	0.5270(6)	13	0.02
	^{35}Cl	18971.55(4)		0.5356(7)		
$2_0^9 3_0^1$	^{37}Cl	19062.44(4)	—	0.5265(15)	10	0.03
	^{35}Cl	19073.98(4)		0.5347(10)		
$1_0^1 2_0^8$	^{37}Cl	—	—	—	9	0.02
	^{35}Cl	19634.30(3)		0.5361(5)		
2_0^{11}	^{37}Cl	19631.70(3)	—	0.5327(7)	12	0.02
	^{35}Cl	19639.20(4)		0.5421(7)		
$2_0^{10} 3_0^1$	^{37}Cl	19774.99(13)	—	0.5320(41)	6	0.06
	^{35}Cl	19787.42(5)		0.5377(12)		
$1_0^1 2_0^7 3_0^1$	^{37}Cl	19864.54(5)	—	0.5222(12)	11	0.03
	^{35}Cl	19873.36(3)		0.5313(8)		
$2_0^9 3_0^2$	^{37}Cl	19932.25(3)	—	0.5242(6)	13	0.02
	^{35}Cl	19949.19(7)		0.5307(31)		

^a Three standard errors given in parenthesis.

^b From Ref. [31].

^c Number of transitions included in the fit.

^d Standard deviation of the fit.

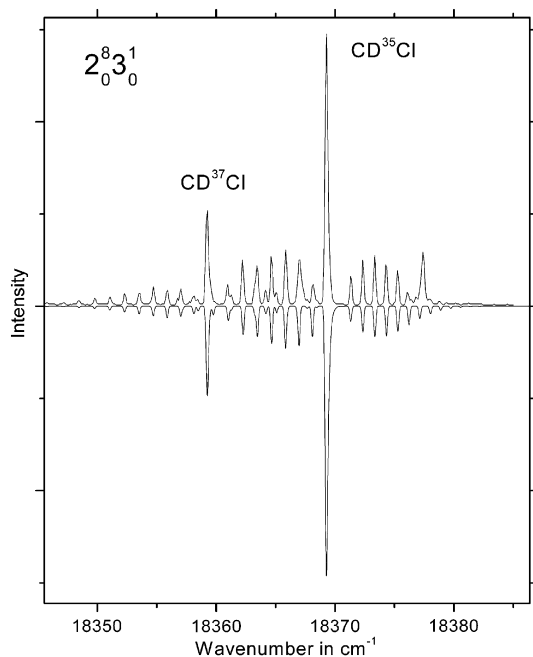


Fig. 2. Fluorescence excitation spectrum (upper) and simulation of the $2_0^8 3_0^1$ band in the $\bar{A}^1 A'' \leftarrow \bar{X}^1 A'$ system of CDCl . The simulation is based upon the rotational constants given in Table 1. The feature in the experimental spectrum at $\sim 18377.5 \text{ cm}^{-1}$ is the nominally forbidden (weakly allowed via axis switching) $^9 Q_0$ subband of the ^{35}Cl isotopomer, which was not included in the simulation. The corresponding ^{37}Cl isotopomer subband cannot be clearly seen due to overlap.

energies calculated by Yu et al. [31] and Fig. 2 displays a comparison of experimental and simulated spectra for the $2_0^8 3_0^1$ band. For each band we typically determined band origins and effective rotational constants $\bar{B}' = 1/2(B' + C')$ for both chlorine isotopomers (^{35}Cl , ^{37}Cl); however, due to the limited range of J in our jet-cooled spectra ($T_{\text{rot}} \sim 15\text{--}20 \text{ K}$), the small ($\sim 10^{-6}$) centrifugal distortion constant D_J was not well determined and was set to zero in the fits.

Most of the bands reported in Table 1 are observed here for the first time. Comparing our results with previous work, we note that Merer and Travis only observed bands in the pure bending progression for CDCl [9]. Recently, Chang and co-workers claimed the first observation of a combination band in this system, reporting a band at $\sim 16,220 \text{ cm}^{-1}$ which was tentatively assigned to $2_0^5 3_0^1$ [42]. In contrast, our results show that $2_0^5 3_0^1$ lies much higher ($\sim 16,338 \text{ cm}^{-1}$); this assignment was confirmed by our observation of other members of this progression, and the excited state isotope shifts, as described below. Based upon the term energies derived from our excitation and emission spectra, we reassign the band observed by Chang and co-workers to the $2_0^6 3_0^1$ hot band.

As mentioned above, we observe extensive activity in the $1_0^1 2_0^n$ progression in addition to the C–D stretching fundamental (1_0^1). These assignments were confirmed by the excited state isotope splittings and SVL emission spectroscopy, as described below. The increased intensity of these

combination bands relative to those in CHCl may arise from increasing mixing among the normal modes caused by the heavier D atom; however, we cannot offer an explanation for why these bands were not observed in previous studies [9,28,40,42]. The anharmonic C–D stretching frequency was determined as $\nu_1' = 2229.6 \text{ cm}^{-1}$, in excellent agreement with that (2232.1 cm^{-1}) predicted at the MRCI/cc-pVTZ level [31].

Fig. 3 displays Dixon plots [57] of the vibrational intervals for the 2^n , $2^n 3^1$, and $1^1 2^n$ progressions, combining our data with the term energy of the 2_0^1 band reported by Sears and co-workers [28]. In these plots we used the average term energy of the two Cl isotopomers for each band, and a minimum indicating the position of the barrier to linearity is clearly observed. Following the procedure used in our previous studies [8,52–54], the data were fit to a third order polynomial using a nonlinear least squares routine, and the minimum position located by differentiation. The fit results are shown as the dashed lines in Fig. 2, and the derived barrier heights relative to the vibrationless level of the $\bar{A}^1 A''$ state are: 2^n , 2140 cm^{-1} ; $2^n 3^1$, 3120 cm^{-1} ; and $1^1 2^n$, 4610 cm^{-1} ; the estimated uncertainties are $\pm 100 \text{ cm}^{-1}$ in each case. Within the fit uncertainties, the increase in barrier height for the $2^n 3^1$ and $1^1 2^n$ progressions is roughly similar to the corresponding fundamental frequencies, indicating little change in bending potential upon excitation of the C–F or C–H stretch [54].

Fig. 4 displays a plot of the excited state ^{35}Cl – ^{37}Cl isotope splitting for the $2^n, 2^n 3^1$, and $1^1 2^n$ bands. As found for CHCl [53], the excited state isotope splittings exhibit a strong dependence on bending quantum number (n), but

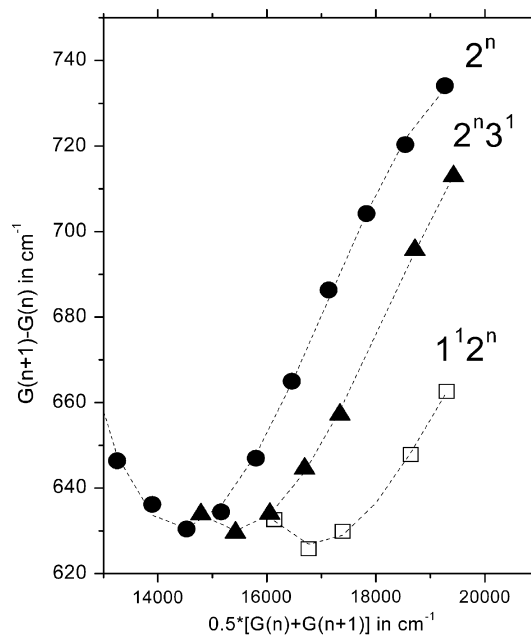


Fig. 3. Dixon plot of the vibrational intervals for the 2^n , $2^n 3^1$, and $1^1 2^n$ progressions. The fits to a third-order polynomial in each case are shown as the dashed lines. The plot for the 2^n progression combines our data with the term energy of the 2_0^1 band reported in Ref. [28].

are significantly larger for the $2^n 3^1$ progression as expected [8,53,54]. Moreover, the isotope splittings reveal a local interaction between $1^1 2^5$ and $2^7 3^1$, and, to a lesser extent, $1^1 2^6$ and $2^8 3^1$. Using a two-level deperturbation scheme,[46,48] we derive a mixing element of $\sim 15 \text{ cm}^{-1}$ for the interaction between $1^1 2^5$ and $2^7 3^1$.

2.2. SVL emission spectra

Single vibronic level (SVL) emission spectra were acquired for CD^{35}Cl from the \tilde{A} state levels: 2^6 , 2^7 , $2^6 3^1$, 2^{11} , $2^{10} 3^1$, $2^9 3^2$, $1^1 2^2$, $1^1 2^4$, $1^1 2^8$, and $1^1 2^7 3^1$; and for CD^{37}Cl from the levels: 2^6 , 2^7 , $2^6 3^1$, 2^{11} , $2^{10} 3^1$, $2^9 3^2$, $1^1 2^2$ and $1^1 2^7 3^1$. Example spectra are shown, along with the discharge background in each case, in Fig. 5. The various spectra allow us to maximize the number of \tilde{X} and \tilde{a} state levels observed, and eliminate spurious lines due the discharge background or collision-induced relaxation in the \tilde{A} state. Here, as in our CHCl study [53], the discharge background was negligible (Fig. 5). The derived \tilde{X} and \tilde{a} state term energies for CD^{35}Cl (Table 2) are in excellent agreement with previous work from Lin et al. [42], although we observe more than twice as many levels; note that for simplicity in Table 2 we use the notation (v_1, v_2, v_3) to label the vibrational states. The experimental errors given in Table 2 reflect the observed standard deviation from the average values calculated from different emission spectra. As in previous studies of CHBr , CDBr , and CHCl [8,53,54], the term energies were derived from SVL emission spectra that show predominantly $K'_a = 0 \rightarrow K''_a = 1$ transitions, and there is thus a small bias in term energies for excited bending levels due to the increase in A rotational constant with bending exci-

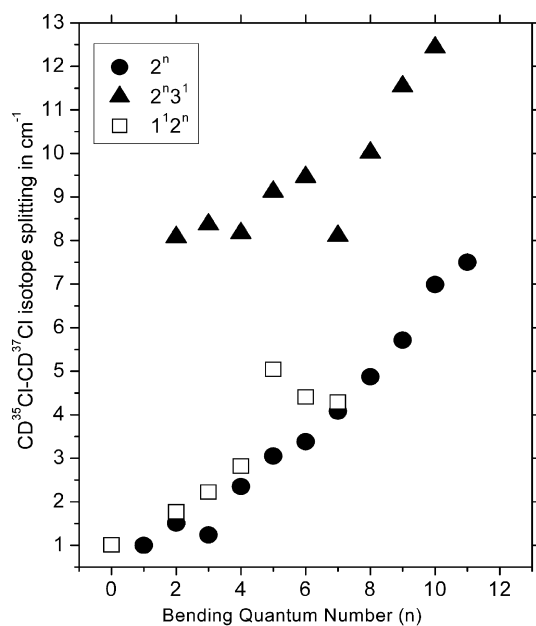


Fig. 4. Excited state ^{35}Cl – ^{37}Cl isotope splitting for all observed 2^n , $2^n 3^1$ and $1^1 2^n$ bands plotted as a function of n .

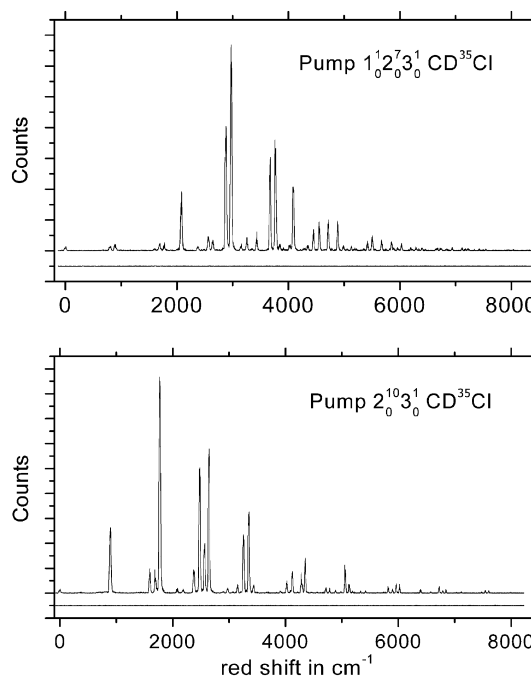


Fig. 5. Single vibronic level emission spectra from the $2^{10} 3^1$ and $1^1 2^7 3^1$ levels of CD^{35}Cl . The x -axis labels the shift in wavenumber from the excitation line, and the discharge background is shown as the lower trace in each panel.

tation, which was not explicitly accounted for in our analysis.

Following our previous work [8,50,53,54], we began by fitting the observed CD^{35}Cl and CD^{37}Cl term energies, using a nonlinear least square routine, to a standard anharmonic potential function (Dunham expansion) of the form [58]:

$$G(v_1, v_2, v_3) = \sum_{i=1}^3 (v_i + 1/2) \omega_i + \sum_{j \geq i=1}^3 (v_i + 1/2)(v_j + 1/2) x_{ij} \quad (1)$$

where ω_i is the harmonic frequency of mode i , x_{ii} is a diagonal anharmonicity constant, and x_{ij} is an off-diagonal or cross-anharmonicity constant. Table 2 gives the experimental CD^{35}Cl term energies and deviations for the Dunham expansion fit, as well as those obtained by comparing our term energies with the results of two recent *ab initio* studies [31,55]. The MRCI/aug-cc-pVTZ calculations of Yu et al. [31] were reported with and without including spin-orbit coupling, while Tarczay et al. [55] reported a more comprehensive set of anharmonic term energies based on a complete quartic force field in internal coordinates computed at CCSD(T)/aug-cc-pVQZ level using second-order vibrational perturbation theory (VPT2) and variational methods (VAR4, VAR4⁺), without including spin-orbit effects.

The standard deviation of the Dunham expansion fit to 47 levels of the CD^{35}Cl isotopomer is 2.5 cm^{-1} , which can be compared to our experimental uncertainty of $\sim 2 \text{ cm}^{-1}$ and the corresponding fit deviation for CH^{35}Cl of

Table 2
Vibrational term energies (in cm^{-1}) for the X^1A' and \tilde{a}^3A'' states of CD^{35}Cl derived from SVL emission spectra. Assignments and deviations from the calculations of Refs. [31] and [55] and a Dunham expansion fit (this work) are given

Term energy		Assignment	Deviations (obs. – calc.)					
This work ^a	Ref. [42]		This work		Ref. [31]		Ref. [55]	
			DE		n.s. ^b	w.s. ^c	VPT2	Var4
801(1)	801	$\tilde{X}(0,0,1)$	–1	–1	–1	3	2	2
893(2)	893	$\tilde{X}(0,1,0)$	2	5	5	–2	–3	–3
1593(4)	1594	$\tilde{X}(0,0,2)$	–2	–2	–2	7	3	3
1691(1)	1690	$\tilde{X}(0,1,1)$	3	3	4	3	0	0
1772(1)	1772	$\tilde{X}(0,2,0)$	1	3	5	–5	–7	–7
2082(2)	2081	$\tilde{X}(1,0,0)$	–1	4	4	8	6	6
2187(2)	2187	$\tilde{a}(0,0,0)$	—	19	18	0	0	0
2375(2)	2377	$\tilde{X}(0,0,3)$	–2	–5	–5	10	5	5
2477(5)	2478	$\tilde{X}(0,1,2)$	1	3	4	4	0	0
2565(2)	2565	$\tilde{X}(0,2,1)$	1	2	4	–1	–6	–5
2644(2)	2644	$\tilde{X}(0,3,0)$	2	5	4	–1	–7	–6
2880(1)	2880	$\tilde{X}(1,0,1)$	–2	5	5	9	6	6
2975(3)	2975	$\tilde{X}(1,1,0)$	3	10	10	4	2	2
3070(3)	—	$\tilde{a}(0,0,1)$	—	–40	–39	7	4	4
3150(2)	—	$\tilde{X}(0,0,4)$	–1	–7	–7	16	8	8
3255(6)	—	$\tilde{X}(0,1,3)$	1	5	5	7	1	1
3348(4)	3349	$\tilde{X}(0,2,2)$	1	4	5	2	–4	–3
3435(2)	3434	$\tilde{X}(0,3,1)$	5	7	5	4	–3	–2
3498(2)	3497	$\tilde{X}(0,4,0)$	–5	–7	1	–3	–16	–13
3602(3)	3601	$\tilde{a}(0,2,0)$	—	60	49	–7	–5	–7
3670(4)	—	$\tilde{X}(1,0,2)$	–1	—	—	12	8	8
3771(3)	3768	$\tilde{X}(1,1,1)$	4	—	—	8	4	4
3850(3)	3850	$\tilde{X}(1,2,0)$	–1	—	—	–4	–2	–1
3912(2)	—	$\tilde{X}(0,0,5)$	–3	—	—	18	7	7
4024(2)	—	$\tilde{X}(0,1,4)$	2	—	—	12	4	4
4092(7)	—	$\tilde{X}(2,0,0)$	2	—	—	17	8	8
4121(2)	—	$\tilde{X}(0,2,3)$	2	—	—	4	–2	–2
—	4214	$\tilde{X}(0,3,2)$	—	—	—	7	1	0
4283(2)	4278	$\tilde{X}(0,4,1)$	–2	—	—	10	–13	–10
4295(2)	4297	$\tilde{a}(0,3,0)$	—	—	—	–5	–7	–13
4351(2)	4350	$\tilde{X}(0,5,0)$	–2	—	—	–5	–16	–11
4452(2)	—	$\tilde{X}(1,0,3)$	0	—	—	17	10	10
4552(4)	—	$\tilde{X}(1,1,2)$	1	—	—	6	2	2
4643(6)	4641	$\tilde{X}(1,2,1)$	2	—	—	2	1	2
4717(3)	4715	$\tilde{X}(1,3,0)$	–4	—	—	11	1	2
4784(3)	—	$\tilde{X}(0,1,5)$	2	—	—	15	6	6
4887(2)	—	$\tilde{X}(2,0,1)$	3	—	—	17	9	9
5057(3)	—	$\tilde{X}(0,4,2)$	–1	—	—	—	—	—
5130(3)	—	$\tilde{X}(0,5,1)$	0	—	—	—	—	—
5192(2)	—	$\tilde{X}(0,6,0)$	–1	—	—	—	—	—
5329(4)	—	$\tilde{X}(1,1,3)$	2	—	—	—	—	—
5353(4)	—	$\tilde{a}(1,0,1)$	—	—	—	0	–4	–4
5419(4)	—	$\tilde{X}(1,2,2)$	–2	—	—	—	—	—
5502(5)	—	$\tilde{X}(1,3,1)$	–3	—	—	—	—	—
5672(3)	—	$\tilde{X}(2,0,2)$	–2	—	—	—	—	—
5823(3)	—	$\tilde{X}(0,4,3)$	1	—	—	—	—	—
5851(3)	—	$\tilde{X}(2,2,0)$	–6	—	—	—	—	—
5895(5)	—	$\tilde{X}(0,5,2)$	–4	—	—	—	—	—
5963(1)	—	$\tilde{X}(0,6,1)$	–3	—	—	—	—	—
6026(3)	—	$\tilde{X}(0,7,0)$	3	—	—	—	—	—
6193(3)	—	$\tilde{X}(1,2,3)$	1	—	—	—	—	—
6730(2)	—	$\tilde{X}(2,3,0)$	5	—	—	—	—	—
6845(3)	—	$\tilde{X}(0,8,0)$	2	—	—	—	—	—
Standard deviations			2.5	16.9	14.8	7.1	6.6	6.3

^a Experimental error (one standard deviation) given in parenthesis (right justified).

^b n.s. = no spin–orbit interaction.

^c w.s. = with spin–orbit interaction.

$\sim 5 \text{ cm}^{-1}$ [53]. The calculations of Yu et al. [31] with and without incorporation of spin orbit coupling, respectively, give overall deviations of 16.9 and 14.8 cm^{-1} , respectively, comparing 17 \tilde{X} and 3 \tilde{a} state levels. For the calculations of Tarczay et al. [55], we find overall deviations of, respectively, 7.1, 6.6, and 6.3 cm^{-1} for the VPT2, VAR4, and VAR4⁺ methods, comparing our term energies to a larger set of 32 \tilde{X} and 5 \tilde{a} state levels. A comparison of experiment and theory for the CD³⁷Cl term energies is available in [Supplementary information](#).

As in the other monohalocarbenes, the triplet levels primarily interact with bending levels in the singlet manifold due to favorable vibrational overlap, although in this case the triplet origin lies almost exactly between $\tilde{X}(0, 2, 0)$ and $\tilde{X}(0, 3, 0)$ [31,42]. At higher energies, the Dunham fit shows that $\tilde{X}(0, 4, 0)$ is shifted down by -5 cm^{-1} due to interaction with the nearby $\tilde{a}(0, 2, 0)$ level; this is in good agreement with the -7 cm^{-1} shift predicted from the MRCI calculations of Yu et al. [31]. Using a two-level deperturbation analysis, we derive a spin-orbit matrix element of $\sim 21 \text{ cm}^{-1}$ for this interaction. At higher energies the mixing becomes extensive, and a number of unassigned lines remain above $\sim 6500 \text{ cm}^{-1}$. Future work will combine our extensive data sets for CDCl and CHCl in a more global deperturbation analysis to obtain additional information on spin-orbit coupling in this system.

The experimentally derived vibrational parameters of the \tilde{X} state are compared in Table 3 with the results of Tarczay et al. [55] and our own Density Functional Theory (DFT) calculations at the B3LYP/aug-cc-pVTZ level, which well reproduced experimental harmonic frequencies in the \tilde{X} state for CHF, CDF, CHCl, CHBr, and CDBr [8,50,52–54]. The calculations were performed using the Gaussian 98 electronic structure package [59] on a personal computer. The calculated frequencies are in good agreement with previous *ab initio* values and with experiment. The optimized geometrical parameters at the B3LYP/aug-cc-pVTZ level [$R_{\text{CCl}} = 1.69 \text{ \AA}$, $R_{\text{CD}} = 1.11 \text{ \AA}$, $\theta = 102.2^\circ$] are in excellent agreement with previous CCSD(T)/aug-cc-pCVQZ studies ($R_{\text{CCl}} = 1.70 \text{ \AA}$, $R_{\text{CD}} = 1.11 \text{ \AA}$, $\theta = 102.3^\circ$) [55].

Table 3
Comparison of calculated CD³⁵Cl/CD³⁷Cl vibrational parameters with those determined from the Dunham expansion fits

Parameter	CD ³⁵ Cl			CD ³⁷ Cl	
	Dunham fit	Ref. [55]	DFT ^a	Dunham fit	DFT ^a
ω_1	2158.9(37)	2148.50	2142.5	2160.7(36)	2142.5
ω_2	904.1(10)	909.14	908.7	904.0(9)	908.2
ω_3	815.2(14)	809.94	783.0	812.8(14)	777.0
x_{11}	-37.3(11)	-37.09		-38.5(11)	
x_{12}	-1.28(51)	1.49		-1.22(55)	
x_{13}	-2.74(64)	-1.39		-3.23(71)	
x_{22}	-5.08(10)	-6.50		-5.12(10)	
x_{23}	-4.86(21)	-4.12		-4.92(21)	
x_{33}	-4.74(23)	-4.74		-5.37(24)	

^a Calculated at the B3LYP/aug-cc-pVTZ level.

3. Conclusions

We have reported extensive fluorescence excitation and single vibronic level emission spectra of the $\tilde{A}^1A'' \leftrightarrow \tilde{X}^1A'$ system of CDCl in the 500–740 nm region, measured under jet-cooled conditions using a pulsed discharge nozzle. In contrast to CHCl, extensive activity in the progressions $2_0^3 3_0^1$ and $1_0^1 2_0^n$ are observed, and a total of 29 cold bands involving the pure bending levels 2_0^n ($n = 2-11$), C–D stretching fundamental (1_0^1), and combination bands $2_0^n 3_0^1$ ($n = 2-10$), $2_0^n 3_0^2$ ($n = 9$), $1_0^1 2_0^n$ ($n = 2-8$), and $1_0^1 2_0^n 3_0^1$ ($n = 7$) were recorded. Most of these were reported here for the first time, and rotational analysis typically yielded band origins and rotational constants for both chlorine isotopomers (CD³⁵Cl, CD³⁷Cl). The derived \tilde{A}^1A'' vibrational intervals were used to determine excited state barriers to linearity for the 2^n , $2^n 3^1$, and $1^1 2^n$ progressions. The \tilde{A}^1A'' state C–D stretching frequency (2229.6 cm^{-1}) is determined here for the first time, in excellent agreement with the MRCI calculations of Yu et al. [31].

Following our observation of new bands in this system, we obtained single vibronic level (SVL) emission spectra which probed the vibrational structure of the \tilde{X}^1A' state up to $\sim 8000 \text{ cm}^{-1}$ above the vibrationless level. The total number of \tilde{X}^1A' and \tilde{a}^3A'' levels observed is more than twice that previously reported. A complete set of Dunham parameters was determined for the \tilde{X}^1A' state of both isotopomers, and comparisons with previous experimental and recent high level *ab initio* studies were reported. Our results have shed new light on the vibrational structure of the \tilde{X}^1A' , \tilde{A}^1A'' , and \tilde{a}^3A'' states of CDCl, and, more generally, spin-orbit coupling in the monohalocarbenes. Future work will combine our extensive data sets for CDCl and CHCl in a global deperturbation analysis to obtain more information on spin-orbit coupling in this system.

Acknowledgment

The National Science Foundation (Grant CHE-0353596) is gratefully acknowledged for support of this research.

Appendix A. Supplementary data

Supplementary data for this article are available on ScienceDirect (www.sciencedirect.com) and as part of the Ohio State University Molecular Spectroscopy Archives (http://msa.lib.ohio-state.edu/jmsa_hp.htm).

References

- [1] R.A. Moss, M. Jones, Jr., (Eds.), Carbenes, Vol. I–II in *Reactive Intermediates in Organic Chemistry Series*, Wiley–Interscience, New York, 1973 (vol. I); 1975 (vol. II).
- [2] W. Kirmse, *Carbene Chemistry*, 2nd ed., Academic, New York, 1971.
- [3] J.C. Sciano, in: *Handbook of Organic Photochemistry*, vol. 2, CRC Press, Boca Raton, FL, 1989, Chapter 9.

- [4] F.A. Carey, R.J. Sundberg, In *Advanced Organic Chemistry, Part 3*, third ed., Plenum, New York, 1990.
- [5] U.E. Weirsum, L.W. Jenneskens, in: Y. Vallée (Ed.), *Gas Phase Reactions in Organic Synthesis*, Gordon and Breach, Amsterdam, The Netherlands, 1997.
- [6] A.M. Dean, J.W. Bozzelli, in: W.C. Gardiner Jr. (Ed.), *Gas-phase Combustion Chemistry*, Springer, New York, 2000, Chapter 2.
- [7] A. Kalemios, T.H. Dunning Jr., A. Mavridis, J.F. Harrison, *Can. J. Chem.* 82 (2004) 684–693.
- [8] M. Deselnicu, C. Mukarakate, C. Tao, S.A. Reid, *J. Chem. Phys.* 124 (2006) 134302/1–134302/11.
- [9] A.J. Merer, D.N. Travis, *Can. J. Phys.* 44 (1966) 525–547.
- [10] A.J. Merer, D.N. Travis, *Can. J. Phys.* 44 (1966) 1541–1550.
- [11] E. Hirota, *Faraday Disc. Chem. Soc.* 74 (1981) 87–95.
- [12] M. Kakimoto, S. Saito, E. Hirota, *J. Mol. Spectrosc.* 88 (1981) 300–310.
- [13] P.H. Mueller, N.G. Rondan, K.N. Houk, J.F. Harrison, D. Hooper, B.H. Willen, J.F. Liebman, *J. Am. Chem. Soc.* 103 (1981) 5049–5052.
- [14] T. Suzuki, S. Saito, E. Hirota, *J. Mol. Spectrosc.* 90 (1981) 447–459.
- [15] M. Kakimoto, S. Saito, E. Hirota, *J. Mol. Spectrosc.* 97 (1983) 194–203.
- [16] R.J. Butcher, S. Saito, E. Hirota, *J. Chem. Phys.* 80 (1984) 4000–4002.
- [17] T. Suzuki, S. Saito, E. Hirota, *Can. J. Phys.* 62 (1984) 1328–1335.
- [18] T. Suzuki, E. Hirota, *J. Chem. Phys.* 85 (1986) 5541–5546.
- [19] B.-C. Chang, T.J. Sears, *J. Chem. Phys.* 102 (1995) 6347–6353.
- [20] B.-C. Chang, T.J. Sears, *J. Mol. Spectrosc.* 173 (1995) 391–403.
- [21] B.-C. Chang, T.J. Sears, *J. Chem. Phys.* 105 (1996) 2135–2140.
- [22] B.-C. Chang, R. Fei, T.J. Sears, *J. Mol. Spectrosc.* 183 (1997) 341–346.
- [23] A.J. Marr, S.W. North, T.J. Sears, L. Ruslen, R.W. Field, *J. Mol. Spectrosc.* 188 (1998) 68–77.
- [24] A.J. Marr, T.J. Sears, *J. Mol. Spectrosc.* 195 (1999) 367–370.
- [25] A.J. Marr, T.J. Sears, *Mol. Phys.* 97 (1999) 185–193.
- [26] B.-C. Chang, M.L. Costen, A.J. Marr, G. Ritchie, G.E. Hall, T.J. Sears, *J. Mol. Spectrosc.* 202 (2000) 131–143.
- [27] H.-G. Yu, T. Lezana-Gonzalez, A.J. Marr, J.T. Muckerman, T.J. Sears, *J. Chem. Phys.* 115 (2001) 5433–5444.
- [28] A. Lin, K. Kobayashi, H.-G. Yu, G.E. Hall, J.T. Muckerman, T.J. Sears, A.J. Merer, *J. Mol. Spectrosc.* 214 (2002) 216–224.
- [29] H.-G. Yu, J.T. Muckerman, T.J. Sears, *J. Chem. Phys.* 116 (2002) 1435–1442.
- [30] B.-C. Chang, J. Guss, T.J. Sears, *J. Mol. Spectrosc.* 219 (2003) 136–144.
- [31] H.-G. Yu, T.J. Sears, J.T. Muckerman, *Mol. Phys.* 104 (2006) 47–53.
- [32] G.E. Hall, T.J. Sears, H.-G. Yu, *J. Mol. Spectrosc.* 235 (2006) 125–131.
- [33] Z. Wang, R.G. Bird, H.-G. Yu, T.J. Sears, *J. Chem. Phys.* 124 (2006) 074314/1–074314/7.
- [34] T.W. Schmidt, G.B. Bacskay, S.H. Kable, *Chem. Phys. Lett.* 292 (1998) 80–86.
- [35] T.W. Schmidt, G.B. Bacskay, S.H. Kable, *J. Chem. Phys.* 110 (1999) 11277–11285.
- [36] K. Nauta, J.S. Guss, N.L. Owens, S.H. Kable, *J. Chem. Phys.* 120 (2004) 3517–3518.
- [37] C.-W. Chen, T.-C. Tsai, B.-C. Chang, *Chem. Phys. Lett.* 347 (2001) 73–78.
- [38] C.-W. Chen, T.-C. Tsai, B.-C. Chang, *J. Mol. Spectrosc.* 209 (2001) 254–258.
- [39] T.-C. Tsai, C.-W. Chen, B.-C. Chang, *J. Chem. Phys.* 115 (2001) 766–770.
- [40] C.-L. Lee, M.-L. Liu, B.-C. Chang, *J. Chem. Phys.* 117 (2002) 3263–3268.
- [41] C.-L. Lee, M.-L. Liu, B.-C. Chang, *Phys. Chem. Chem. Phys.* 5 (2003) 3859–3863.
- [42] C.-S. Lin, Y.-E. Chen, B.-C. Chang, *J. Chem. Phys.* 121 (2004) 4164–4170.
- [43] W.-Z. Chang, H.-J. Hsu, B.-C. Chang, *Chem. Phys. Lett.* 413 (2005) 25–30.
- [44] H. Fan, I. Ionescu, C. Annesley, S.A. Reid, *Chem. Phys. Lett.* 378 (2003) 548–552.
- [45] H. Fan, I. Ionescu, C. Annesley, J. Cummins, M. Bowers, S.A. Reid, *J. Mol. Spectrosc.* 225 (2004) 43–47.
- [46] H. Fan, I. Ionescu, C. Annesley, J. Cummins, M. Bowers, J. Xin, S.A. Reid, *J. Phys. Chem. A* 108 (2004) 3732–3738.
- [47] I. Ionescu, H. Fan, C. Annesley, J. Xin, S.A. Reid, *J. Chem. Phys.* 120 (2004) 1164–1167.
- [48] H. Fan, I. Ionescu, J. Xin, S.A. Reid, *J. Chem. Phys.* 121 (2004) 8869–8873.
- [49] I. Ionescu, H. Fan, E. Ionescu, S.A. Reid, *J. Chem. Phys.* 121 (2004) 8874–8879.
- [50] H. Fan, C. Mukarakate, M. Deselnicu, C. Tao, S.A. Reid, *J. Chem. Phys.* 123 (2005) 014314/1–014314/7.
- [51] E. Ionescu, S.A. Reid, *J. Mol. Struct. THEOCHEM* 725 (2005) 45–53.
- [52] C. Tao, M. Deselnicu, C. Mukarakate, S.A. Reid, *Phys. Chem. Chem. Phys.* 8 (2006) 707–713.
- [53] C. Tao, C. Mukarakate, S.A. Reid, *J. Chem. Phys.* 124 (2006) 224314/1–224314/11.
- [54] C. Tao, M. Deselnicu, C. Mukarakate, S.A. Reid, *J. Chem. Phys.* 125 (2006) 094305/1–094305/9.
- [55] G. Tarczay, T.A. Miller, G. Czako, A.G. Császár, *Phys. Chem. Chem. Phys.* 7 (2005) 2881–2893.
- [56] R.H. Judge, D.J. Clouthier, *Comput. Phys. Commun.* 135 (2001) 293–311.
- [57] R.N. Dixon, *Trans. Faraday Soc.* 60 (1964) 1363–1368.
- [58] G. Herzberg, *Molecular Spectra and Molecular Structure III. Electronic Spectra of Polyatomic Molecules*, Van Nostrand, New York, 1966.
- [59] M.J. Frisch, G.W. Trucks, H.B. Schlegel, et al., *Gaussian 98, Rev. A.111.4*, Gaussian, Inc., Pittsburgh, PA, 2002.